

The Landau Pole and Z' decays in the 331 bilepton model

R. Martínez* and F. Ochoa†

Departamento de Física, Universidad Nacional,
Bogotá-Colombia

29th November 2017

Abstract

We calculate the decay widths and branching ratios of the extra neutral boson Z' predicted by the 331 bilepton model in the framework of two different particle contents. These calculations are performed taken into account oblique radiative corrections, and Flavor Changing Neutral Currents (FCNC) under the ansatz of Matsuda as a texture for the quark mass matrices. Contributions of the order of $10^{-1} - 10^{-2}$ are obtained in the branching ratios, and partial widths about one order of magnitude bigger in relation with other non- and bilepton models are also obtained. A Landau-like pole arise at 3.5 TeV considering the full particle content of the minimal model (MM), where the exotic sector is considered as a degenerated spectrum at 3 TeV scale. The Landau pole problem can be avoid at the TeV scales if a new leptonic content running below the threshold at 3 TeV is implemented as suggested by other authors.

1 Introduction

The models with gauge symmetry $SU(3)_c \otimes SU(3)_L \otimes U(1)_X$, also called 331 models, arise by enlarging the symmetry group where the Standar Model (SM) is embedded as an effective theory at low energy. Based on the criterion of cancellation of chiral anomalies [1], these models have generated new expectations and possibilities of new physics at the TeV scale whose predictions are sensitive to experimental observation and will be of great interest in the next generation of colliders (LHC, ILC) [2] at the TeV energy scales. Among the most remarkable features of these models, we have that they arise as an interesting alternative to explain the origin of generations [3], they leads to the prediction of new neutral and charged vector bosons with observable consequences at low and high energies, and they can predict the charge quantization for a three family model even when neutrino masses are added [4].

*e-mail: remartinezm@unal.edu.co

†e-mail: faochoap@unal.edu.co

Although cancellation of anomalies leads to some required conditions [5], such criterion alone still permits an infinite number of 331 models. In these models, the electric charge is defined in general as a linear combination of the diagonal generators of the group

$$Q = T_3 + \beta T_8 + XI, \quad (1)$$

where the value of the β parameter determines the fermion assignment and, more specifically, the electric charges of the exotic spectrum. Hence, it is customary to use this quantum number to classify the different 331 models. There are two main versions of 331 models corresponding to $\beta = -1/\sqrt{3}$ [5, 6] which leads to non-exotic charges, and $\beta = -\sqrt{3}$ [7] which accounts for doubly charged bilepton bosons. An extensive and detailed study of models with β arbitrary have been carried out in ref. [8] for the scalar sector and in ref. [9] for the fermionic and gauge sector.

The group structure of these models leads, along with the SM neutral boson Z , to the prediction of an additional current associated to the extra neutral boson Z' . It is possible to obtain constraints through direct production of the Z' boson (for center-of-mass energy $\sqrt{s} \approx M_{Z'} > M_Z$), where the study of decay widths provide information about possible Z' -detection in future experimental measurements. These decay widths are controlled by the $SU(3)_L \otimes U(1)_X$ coupling constants denoted by g_L and g_X , respectively, and which follows the relation

$$\frac{g_X^2}{g_L^2} = \frac{S_W^2}{1 - (1 + \beta^2)S_W^2}, \quad (2)$$

where $S_W = \sin \theta_W$ with θ_W the Weinberg angle. The Eq. 2 exhibit a Landau pole when $S_W^2(\mu) = 1/(1 + \beta^2)$, where the coupling constant g_X becomes infinite, and the models lose their perturbative character at some energy scale μ . In particular, the model with $\beta = -\sqrt{3}$ shows a Landau pole when $S_W^2 = 1/4$ at the scale $\mu \approx 4$ TeV, which is near to the bounds associated to the Z' -mass predicted by this model [10]. Thus, this version of the 331 models points to a nonperturbative regime at the Z' peak. This problem has already been considered in ref. [11] with and without supersymmetry of the bilepton model. In particular, a possible solution of this puzzle was proposed in ref. [12] by introducing an additional particle content, which change the behaviour of the running Weinberg angle and restores the perturbative feature of the model. The new particle content is composed by three exotic lepton triplets, one exotic scalar triplet and two exotic scalar doublets. In this extended model (EM), the usual exotic particles predicted by the minimal 331 model (MM) remains as heavy particles which are decoupled below the scale μ_{331} where the symmetry breaking $SU(3)_L \times U(1)_X \rightarrow SU(2)_L \times U(1)_Y$ takes place, so that they are not considered as active degrees of freedom below the Z' energy scale. However, some phenomenological studies estimates that the exotic quarks have a mass in the range 1.5 – 4 TeV [13], and they could enter as active degree of freedom at the Z' scale.

In this work we study the behaviour of the running Weinberg angle for different particle content in the 331 bilepton model, where the exotic particles define a new threshold energy scale below $M_{Z'}$. Later, we obtain the partial widths and the branching decays of the Z' boson in the 331 bilepton model for two perturbative particle content, where the running coupling constants at $M_{Z'}$ scale is taken into account in agreement with the new particle

content. This paper is organized as follows. Subsection 2.1 is devoted to summarize the minimal 331 bilepton model (MM) and the behaviour of the running Weinberg angle. In Subsec. 2.2, we indicate the most remarkable features of the extended 331 bilepton model (EM) in order to obtain a decreasing running Weinberg angle. In Subsec. 2.3, we consider a modified extended 331 bilepton model (MEM), where we include the exotic spectrum of the minimal model as active degree of freedom below the Z' scale. Finally, in Sec. 3 we calculate de partial decays and branching ratios of the Z' boson in the framework of the EM and MEM bilepton models, where effects of Flavor Changing Neutral Currents (FCNC) and oblique radiative corrections are taken into account.

2 Perturbative and nonperturbative bilepton models

In this section we show different particle contents in the 331 bilepton model, which control the behavior of the Weinberg angle and the coupling constants with the increasing of the energy.

2.1 The minimal 331 bilepton model (MM)

The minimal 331 fermionic structure for three families is shown in table 1 for the bilepton model corresponding to $\beta = -\sqrt{3}$, where all leptons transform as $(\mathbf{1}, \mathbf{3}, \mathbf{X}_\ell^L)$ and $(\mathbf{1}, \mathbf{1}, \mathbf{X}_{\ell'}^R)$ under $(SU(3)_c, SU(3)_L, U(1)_X)$, with \mathbf{X}_ℓ^L and $\mathbf{X}_{\ell'}^R$ the $U(1)_X$ values associated to the left- and right-handed leptons, respectively; while the quarks transform as $(\mathbf{3}, \mathbf{3}^*, \mathbf{X}_{q_m^*}^L)$, $(\mathbf{3}^*, \mathbf{1}, \mathbf{X}_{q_m'}^R)$ for the first two families, and $(\mathbf{3}, \mathbf{3}, \mathbf{X}_{q_3}^L)$, $(\mathbf{3}^*, \mathbf{1}, \mathbf{X}_{q_3}^R)$ for the third family, where $\mathbf{X}_{q_m^*}^L$, $\mathbf{X}_{q_3}^L$ and $\mathbf{X}_{q_m'}^R$, $\mathbf{X}_{q_3}^R$ correspond to the $U(1)_X$ values for left- and right-handed quarks. We denote $\mathbf{X}_{q_3}^L$ and $\mathbf{X}_{q_m^*}^L$ as the values associated to the $SU(3)_L$ space under representation $\mathbf{3}$ and $\mathbf{3}^*$, respectively. The quantum numbers \mathbf{X}_ψ for each representation are given in the third column from table 1, where the definition of the electric charge in Eq. 1 has been used, demanding charges of 2/3 and $-1/3$ to the up- and down-type quarks, respectively, and charges of -1,0 for the charged and neutral leptons. We recognize three different possibilities to assign the physical quarks in each family representation as shown in table 2 [14]. At low energy, the three models from table 2 are equivalent and there are not any phenomenological feature that allow us to detect differences between them. In fact, they must reduce to the SM which is an universal family model in $SU(2)_L$. However, through the couplings of the three families to the additional neutral current (Z') and the introduction of a mixing angle between Z and Z' , it is possible to recognize differences among the three models at the electroweak scale [10, 15].

For the scalar sector described by Table 3, we introduce the triplet field χ with vacuum expectation value (VEV) $\langle \chi \rangle^T = (0, 0, \nu_\chi)$, which induces the masses to the third fermionic components. In the second transition it is necessary to introduce two triplets ρ and η with VEV $\langle \rho \rangle^T = (0, \nu_\rho, 0)$ and $\langle \eta \rangle^T = (\nu_\eta, 0, 0)$ in order to give masses to the quarks of type up and down, respectively.

In the gauge boson spectrum associated with the group $SU(3)_L \otimes U(1)_X$, we have the

representation	Q_ψ	X_ψ
$q_{m^*L} = \begin{pmatrix} d_{m^*} \\ -u_{m^*} \\ J_{m^*} \end{pmatrix}_L : \mathbf{3}^*$	$\begin{pmatrix} -1/3 \\ 2/3 \\ -4/3 \end{pmatrix}$	$-1/3$
$d_{m^*R}; u_{m^*R}; J_{m^*R} : \mathbf{1}$	$-1/3; 2/3; -4/3$	$-1/3, 2/3, -4/3$
$q_{3L} = \begin{pmatrix} u_3 \\ d_3 \\ J_3 \end{pmatrix}_L : \mathbf{3}$	$\begin{pmatrix} 2/3 \\ -1/3 \\ 5/3 \end{pmatrix}$	$2/3$
$u_{3R}; d_{3R}; J_{3R} : \mathbf{1}$	$2/3; -1/3; 5/3$	$2/3, -1/3, 5/3$
$\ell_{jL} = \begin{pmatrix} \nu_j \\ e_j \\ E_j^+ \end{pmatrix}_L : \mathbf{3}$	$\begin{pmatrix} 0 \\ -1 \\ 1 \end{pmatrix}$	0
$e_{jR}; E_{jR}^{-Q_1}$	$-1; 1$	$-1, 1$

Table 1: Fermionic content for three generations with $\beta = -\sqrt{3}$. We take $m^* = 1, 2$, and $j = 1, 2, 3$

Representation A	Representation B	Representation C
$q_{mL} = \begin{pmatrix} d, s \\ -u, -c \\ J_1, J_2 \end{pmatrix}_L : \mathbf{3}^*$	$q_{mL} = \begin{pmatrix} d, b \\ -u, -t \\ J_1, J_3 \end{pmatrix}_L : \mathbf{3}^*$	$q_{mL} = \begin{pmatrix} s, b \\ -c, -t \\ J_2, J_3 \end{pmatrix}_L : \mathbf{3}^*$
$q_{3L} = \begin{pmatrix} t \\ b \\ J_3 \end{pmatrix}_L : \mathbf{3}$	$q_{3L} = \begin{pmatrix} c \\ s \\ J_2 \end{pmatrix}_L : \mathbf{3}$	$q_{3L} = \begin{pmatrix} u \\ d \\ J_1 \end{pmatrix}_L : \mathbf{3}$

Table 2: Three different assignments for the $SU(3)_L$ family representation of quarks

	Q_Φ	X_Φ
$\chi = \begin{pmatrix} \chi_1^- \\ \chi_2^- \\ \xi_\chi + \nu_\chi \pm i\zeta_\chi \end{pmatrix}$	$\begin{pmatrix} -1 \\ -2 \\ 0 \end{pmatrix}$	-1
$\rho = \begin{pmatrix} \rho_1^+ \\ \xi_\rho + \nu_\rho \pm i\zeta_\rho \\ \rho_3^{++} \end{pmatrix}$	$\begin{pmatrix} 1 \\ 0 \\ 2 \end{pmatrix}$	1
$\eta = \begin{pmatrix} \xi_\eta + \nu_\eta \pm i\zeta_\eta \\ \eta_2^- \\ \eta_3^+ \end{pmatrix}$	$\begin{pmatrix} 0 \\ -1 \\ 1 \end{pmatrix}$	0

Table 3: *Scalar spectrum that break the 331 symmetry and give masses to the fermions.*

charged sector

$$W_\mu^\pm = \frac{1}{\sqrt{2}} (W_\mu^1 \mp iW_\mu^2) ; K_\mu^{\pm 1} = \frac{1}{\sqrt{2}} (W_\mu^4 \mp iW_\mu^5) ; K_\mu^{\pm 2} = \frac{1}{\sqrt{2}} (W_\mu^6 \mp iW_\mu^7) \quad (3)$$

and the neutral sector that corresponds to the photon, the Z and the Z' bosons

$$\begin{aligned} A_\mu &= S_W W_\mu^3 + C_W \left(-\sqrt{3}T_W W_\mu^8 + \sqrt{1 - 3T_W^2} B_\mu \right), \\ Z_\mu &= C_W W_\mu^3 - S_W \left(-\sqrt{3}T_W W_\mu^8 + \sqrt{1 - 3T_W^2} B_\mu \right), \\ Z'_\mu &= -\sqrt{1 - 3T_W^2} W_\mu^8 - \sqrt{3}T_W B_\mu, \end{aligned} \quad (4)$$

where the Weinberg angle is defined as

$$S_W = \sin \theta_W = \frac{g_X}{\sqrt{g_L^2 + 4g_X^2}}, \quad T_W = \tan \theta_W = \frac{g_X}{\sqrt{g_L^2 + 3g_X^2}} \quad (5)$$

Further, a small mixing angle between the two neutral currents Z_μ and Z'_μ appears with the following mass eigenstates [9]

$$\begin{aligned} Z_{1\mu} &= Z_\mu C_\theta + Z'_\mu S_\theta; \quad Z_{2\mu} = -Z_\mu S_\theta + Z'_\mu C_\theta; \\ \tan \theta &= \frac{1}{\Lambda + \sqrt{\Lambda^2 + 1}}; \quad \Lambda = \frac{-2S_W C_W^2 g_X^2 \nu_\chi^2 + \frac{3}{2} S_W T_W^2 g_L^2 (\nu_\eta^2 + \nu_\rho^2)}{g_L g_X T_W^2 [-3\sqrt{3} S_W^2 (\nu_\eta^2 + \nu_\rho^2) + C_W^2 (\nu_\eta^2 - \nu_\rho^2)]}. \end{aligned} \quad (6)$$

The solution of the renormalization group at the lowest one-loop order gives the running coupling constant for $\widetilde{M} \leq \mu$

$$g_i^{-2}(\widetilde{M}) = g_i^{-2}(\mu) + \frac{b_i}{8\pi^2} \ln \left(\frac{\mu}{\widetilde{M}} \right), \quad (7)$$

for $i = 1, 2, 3$, each one corresponding to the constant coupling of $U(1)_Y$, $SU(2)_L$ and $SU(3)_c$, respectively. Specifically, we use the matching condition for the constant couplings, where the $SU(3)_L$ constant g_L is the same as the $SU(2)_L$ constant, i.e. $g_2 = g_L$. Running the constants at the scale $\mu = M_{Z'}$, we obtain for $g_1 = g_Y$ and $g_2 = g_L$

$$\begin{aligned} g_Y^2(M_{Z'}) &= \frac{g_Y^2(\widetilde{M})}{1 - \frac{b_1}{8\pi^2} g_Y^2(\widetilde{M}) \ln\left(\frac{M_{Z'}}{\widetilde{M}}\right)} \\ g_L^2(M_{Z'}) &= \frac{g_L^2(\widetilde{M})}{1 - \frac{b_2}{8\pi^2} g_L^2(\widetilde{M}) \ln\left(\frac{M_{Z'}}{\widetilde{M}}\right)} \end{aligned} \quad (8)$$

where the renormalization coefficients for a general $SU(N)$ gauge group are defined by

$$b_i = \frac{2}{3} \sum_{\text{fermions}} \text{Tr}(T_i(F)T_i(F)) + \frac{1}{3} \sum_{\text{scalars}} \text{Tr}(T_i(S)T_i(S)) - \frac{11}{3} C_{2i}(G), \quad (9)$$

with $T_i(I)$ corresponding to the generators of the fermionic (F) or scalar (S) representations. For $SU(N)$, $\text{Tr}(T(I)T(I)) = 1/2$ and $C_2(G) = N$. For $U(1)_Y$, $\text{Tr}(T(I)T(I)) = Y^2$ and $C_2(G) = 0$. With the above definitions, we can obtain the running Weinberg angle at the Z' scale

$$\begin{aligned} S_W^2(M_{Z'}) &= \frac{g_Y^2(M_{Z'})}{g_L^2(M_{Z'}) + g_Y^2(M_{Z'})} \\ &= S_W^2(\widetilde{M}) \left[\frac{1 - \frac{b_2}{2\pi} \alpha_2(\widetilde{M}) \ln\left(\frac{M_{Z'}}{\widetilde{M}}\right)}{1 - \frac{b_1+b_2}{2\pi} \alpha(\widetilde{M}) \ln\left(\frac{M_{Z'}}{\widetilde{M}}\right)} \right]. \end{aligned} \quad (10)$$

The running Weinberg angle depends on the particle content of the model. First, we consider only the particle content of the effective Two Higgs Doublet Model (THDM) below $M_{Z'}$, where the heavy exotic fermions J_{m^*} , J_3 , E_j , the scalar singlets ρ_3^{++} , η_3^+ and the scalar triplet χ in Table 1 are not considered as active degrees of freedom i.e. they are decoupled below the symmetry breaking scale μ_{331} . Thus, the renormalization coefficient takes the values

$$\begin{aligned} b_1 &= \frac{20}{9} N_f + \frac{1}{6} N_H = 7, \\ b_2 &= \frac{4}{3} N_f + \frac{1}{6} N_H - \frac{22}{3} = -3, \end{aligned} \quad (11)$$

where $N_f = 3$ is the number of fermion families and $N_H = 2$ the number of $SU(2)_L$ scalar doublets of the effective THDM. Taking $\widetilde{M} = M_Z$ we run the Eqs. 8 and 10 using the following values at the M_Z scale

$$\begin{aligned}
\alpha_Y^{-1}(M_Z) &= 98.36461 \pm 0.06657; & \alpha^{-1}(M_Z) &= 127.934 \pm 0.027; \\
\alpha_2^{-1}(M_Z) &= 29.56938 \pm 0.00068; & S_W^2(M_Z) &= 0.23113 \pm 0.00015.
\end{aligned}
\tag{12}$$

Fig. 1 display the evolution of the Weinberg angle for the minimal 331 bilepton model. We can see a Landau pole at the energy scale $\mu \approx 4$ TeV, which corresponds to the lowest bound of the Z' mass for the bilepton model, such as studied in ref. [10]. Then, as shown in ref. [11], perturbation theory can not be used at the TeV scale energies in the minimal model even though supersymmetry were implemented.

2.2 The extended 331 bilepton model (EM)

In order to avoid the nonperturbative character of this model at the TeV energies, it was proposed in ref. [12] to introduce an additional exotic particle content, where three lepton triplets with null hypercharge, one scalar triplet with null hypercharge and two scalar doublets with $Y^2 = 9$ remains as new degrees of freedom at energies below the scale μ_{331} in order to obtain a perturbative regime at the Z' energy scale. In this case, the renormalization coefficients take the form [12]

$$\begin{aligned}
b_1 &= \frac{20}{9}N_f + \frac{1}{6}N_H + \frac{Y_S^2}{6}N_S + Y_{TF}^2N_{TF} + \frac{Y_{TS}^2}{4}N_{TS} = 10, \\
b_2 &= \frac{4}{3}N_f + \frac{1}{6}N_H - \frac{22}{3} + \frac{8}{3}N_{TF} + \frac{2}{3}N_{TS} + \frac{1}{6}N_S = 6,
\end{aligned}
\tag{13}$$

with $N_S = 2$ the number of new scalar doublets, $N_{TF} = 3$ the number of new fermionic triplets, and $N_{TS} = 1$ the number of new scalar triplets, each one with the corresponding hypercharge values $Y_S = \pm 3$, $Y_{TF} = 0$ and $Y_{TS} = 0$. In this case, the Weinberg angle runs as shown by Fig. 2 [12] exhibiting a decreasing behavior at the TeV scale. Thus the perturbative character of the model is restored. The new particles are embedded in three octet representations for leptons and one octet for the scalar sector. Thus, there are additional new leptons that can be made heavy through the scalar octet. The $U(1)_X$ quantum number of these new multiplets are null, so that they do not contribute to the anomalies and the cancellation of anomalies is preserved. The Table 4 resumes the new bunch of particles of the extended 331 bilepton model.

2.3 Modification to the extended model (MEM)

In the previous models, the usual exotic spectrum of the MM is considered as heavy particles that are decoupled below the breaking scale μ_{331} and do not participate as active degree of freedom in the renormalization coefficient. However, by comparing the data with radiative corrections to the decay $Z \rightarrow b\bar{b}$ carried out in ref [13], exotic quarks with a mass in the range 1.5 – 4 TeV are found for the 331-bilepton model, which lies in the range below the Z' scale. Then, we take the full 331 spectrum from tables 1 and 3, where the exotic particles are considered as a degenerated spectrum. In agreement with the ref. [13], it is reasonable

		representation
Leptons	$\Xi_a =$	$\begin{pmatrix} \frac{1}{\sqrt{2}}t_a^0 + \frac{1}{\sqrt{6}}\lambda_a^0 & t_a^+ & \delta_a^- \\ t_a^- & \frac{-1}{\sqrt{2}}t_a^0 + \frac{1}{\sqrt{6}}\lambda_a^0 & \delta_a^{--} \\ \xi_a^+ & \xi_a^{++} & \frac{-2}{\sqrt{6}}\lambda_a^0 \end{pmatrix}$
Scalars	$\Sigma =$	$\begin{pmatrix} \frac{1}{\sqrt{2}}\phi^0 + \frac{1}{\sqrt{6}}\varphi^0 & \phi^+ & \varphi_1^- \\ \phi^- & \frac{-1}{\sqrt{2}}\phi^0 + \frac{1}{\sqrt{6}}\varphi^0 & \varphi_1^{--} \\ \varphi_2^+ & \varphi_2^{++} & \frac{-2}{\sqrt{6}}\varphi^0 \end{pmatrix}$

Table 4: *Additional particle content in the extended 331 bilepton model (EM), with $a = 1, 2, 3$ in the lepton sector.*

to estimate $m_{J_j, E_j, \rho_3^{++}, \eta_3^+, \chi_1^-, \chi_2^-} \approx 3 \text{ TeV}$, defining a new running scale. Then, the Weinberg angle evolve from the Z scale in a two stage process. First, below $\mu = 3 \text{ TeV}$, the running parameters evolve as described by Eq. 10 with the coefficients from Eq. 11 of the effective THDM, from where we obtain at 3 TeV that

$$\begin{aligned} \alpha_Y^{-1}(3 \text{ TeV}) &= 94.4724; & \alpha^{-1}(3 \text{ TeV}) &= 125.710; \\ \alpha_2^{-1}(3 \text{ TeV}) &= 31.2374; & S_W^2(3 \text{ TeV}) &= 0.24849. \end{aligned} \quad (14)$$

Later, above the 3 TeV threshold, the spectrum contains the exotic 331 particles with the following coefficients

$$\begin{aligned} b_1 &= \frac{20}{9}N_f + \frac{1}{6}N_H + \frac{2}{3}\sum_{\text{sing.}} Y_f^2 + \frac{1}{3}\sum_{\text{sing}} Y_s^2 + \frac{2}{3}Y_\chi^2 = \frac{79}{2}, \\ b_2 &= \frac{4}{3}N_f + \frac{1}{6}N_H - \frac{43}{3} = -\frac{17}{6}, \end{aligned} \quad (15)$$

with $Y_{f,s}$ the hypercharge of the singlets $f = J_j, E_j$ and $s = \rho_3^{++}, \eta_3^+$, and Y_χ the hypercharge of the doublet (χ_1^-, χ_2^-) . For the second stage, we use the inputs at 3 TeV from Eq. 14. In this way, we obtain the plot shown in Fig. 3. We can see how the behavior of the running angle changes at the 3 TeV scale. The direct consequence to download the exotic 331 spectrum at $3 \text{ TeV} < M_{Z'}$ is that the Weinberg angle increases faster and reaches to the Landau pole at 3.5 TeV below the Z' scale, which can be observe in the Fig. 3. In order to pull this limit, we add into the degenerated exotic spectrum at 3 TeV scale of the EM, the new particle content in Table 4. We obtain the plot displayed in Fig. 4, where the Landau pole is pulled to 3.7 TeV, that, however, does not restore the perturbative behavior near the Z' scale.

On the other hand, we can consider that the extended exotic particles from Tab. 4 runs below the 3 TeV threshold. In this case, the evolution of the coupling constant is controlled by the coefficients in Eq. 13, from where we get the new inputs at the threshold

$$\begin{aligned}\alpha_Y^{-1}(3 \text{ TeV}) &= 92.8048; & \alpha^{-1}(3 \text{ TeV}) &= 119.038; \\ \alpha_2^{-1}(3 \text{ TeV}) &= 26.2334; & S_W^2(3 \text{ TeV}) &= 0.22038.\end{aligned}\quad (16)$$

Above 3 TeV, the full exotic spectrum of the MM is activated, and the renormalization coefficients are defined as the combination of 13 and 15, obtaining $b_1 = 85/2$ and $b_2 = 37/6$. We see in this case that the Landau pole is pulled at very high scales as we can observe in Fig. 5, where the Weinberg angle decreases with the energy until the 3 TeV threshold, from where it begins to increase slowly so that perturbation theory can be applied at the Z' scale. Thus, the Landau pole is pulled beyond the TeV energy scales.

3 The Z' decays in the perturbative models

Decay widths of Z' with and without flavor changing neutral currents are obtained in ref. [15] for models with $\beta = 1/\sqrt{3}$, which displays a Z' mass bound of the order of 1.5 TeV and does not exhibit Landau pole at the TeV energy scale. In this section, we obtain the Z' decay for the bilepton model under the framework of two different particle contents.

In Tab. 2, which is written in weak eigenstates $f^{0(r)}$, we consider linear combinations in each representation $r = A, B, C$ among the three families to obtain couplings in mass eigenstates $f^{(r)}$ through the rotation matrix R_f that diagonalize the Yukawa mass terms, where $f^{0(r)} = R_f f^{(r)}$. Thus, the neutral couplings associated with Z' and the SM-fermions in mass eigenstates can be written as [15]

$$\begin{aligned}\mathcal{L}^{NC} &= \frac{g_L}{2C_W} \{ [\bar{U}\gamma_\mu (\tilde{\mathfrak{g}}_v^{U(r)} - \tilde{\mathfrak{g}}_a^{U(r)}\gamma_5) U + \bar{D}\gamma_\mu (\tilde{\mathfrak{g}}_v^{D(r)} - \tilde{\mathfrak{g}}_a^{D(r)}\gamma_5) D \\ &\quad + \bar{N}\gamma_\mu (\tilde{g}_v^N - \tilde{g}_a^N\gamma_5) N + \bar{E}\gamma_\mu (\tilde{g}_v^E - \tilde{g}_a^E\gamma_5) E] Z'^\mu \},\end{aligned}\quad (17)$$

with $U = (u, c, t)^T$, $D = (d, s, b)^T$, $N = (\nu_e, \nu_\mu, \nu_\tau)^T$, $E = (e, \mu, \tau)^T$, and $\tilde{\mathfrak{g}}_{v,a}^{q(r)} = R_q^\dagger \tilde{g}_{v,a}^{q(r)} R_q$. Thus, we obtain flavor changing couplings in the quark sector due to the matrix R_f . The vector and axial vector couplings of the Z' field are listed in Table 5 for each component.

As discussed in ref. [15], we can adopt the ansatz of Matsuda [16] on the texture of the quark mass matrices with the following rotation matrices

$$R_D = \begin{pmatrix} c & s & 0 \\ -\frac{s}{\sqrt{2}} & \frac{c}{\sqrt{2}} & -\frac{1}{\sqrt{2}} \\ -\frac{s}{\sqrt{2}} & \frac{c}{\sqrt{2}} & \frac{1}{\sqrt{2}} \end{pmatrix}; \quad R_U = \begin{pmatrix} c' & 0 & s' \\ -\frac{s'}{\sqrt{2}} & -\frac{1}{\sqrt{2}} & \frac{c'}{\sqrt{2}} \\ -\frac{s'}{\sqrt{2}} & \frac{1}{\sqrt{2}} & \frac{c'}{\sqrt{2}} \end{pmatrix},\quad (18)$$

with

$$\begin{aligned}c &= \sqrt{\frac{m_s}{m_d + m_s}}; & s &= \sqrt{\frac{m_d}{m_d + m_s}}; \\ c' &= \sqrt{\frac{m_t}{m_t + m_u}}; & s' &= \sqrt{\frac{m_u}{m_t + m_u}}.\end{aligned}\quad (19)$$

<i>Fermion</i>	\tilde{g}_v^f	\tilde{g}_a^f
ν_j	$\frac{-\sqrt{1-4S_W^2}}{2\sqrt{3}}$	$\frac{-\sqrt{1-4S_W^2}}{2\sqrt{3}}$
e_j	$\frac{-1+10S_W^2}{2\sqrt{3}\sqrt{1-4S_W^2}}$	$\frac{-\sqrt{1-4S_W^2}}{2\sqrt{3}}$
E_j	$\frac{1-5S_W^2}{\sqrt{3}\sqrt{1-4S_W^2}}$	$\frac{1-S_W^2}{\sqrt{3}\sqrt{1-4S_W^2}}$
d_{m^*}	$\frac{1}{2\sqrt{3}\sqrt{1-4S_W^2}}$	$\frac{\sqrt{1-4S_W^2}}{2\sqrt{3}}$
u_{m^*}	$\frac{1-6S_W^2}{2\sqrt{3}\sqrt{1-4S_W^2}}$	$\frac{1+2S_W^2}{2\sqrt{3}\sqrt{1-4S_W^2}}$
J_{m^*}	$\frac{-1+9S_W^2}{\sqrt{3}\sqrt{1-4S_W^2}}$	$\frac{-1+S_W^2}{\sqrt{3}\sqrt{1-4S_W^2}}$
u_3	$\frac{-1-4S_W^2}{2\sqrt{3}\sqrt{1-4S_W^2}}$	$\frac{-\sqrt{1-4S_W^2}}{2\sqrt{3}}$
d_3	$\frac{-1+2S_W^2}{2\sqrt{3}\sqrt{1-6S_W^2}}$	$\frac{-1-2S_W^2}{2\sqrt{3}\sqrt{1-4S_W^2}}$
J_3	$\frac{1-11S_W^2}{\sqrt{3}\sqrt{1-4S_W^2}}$	$\frac{1-S_W^2}{\sqrt{3}\sqrt{1-4S_W^2}}$

Table 5: Vector and axial vector couplings of fermions and Z' boson.

where the quark masses at the $M_{Z'}$ scale are

$$\begin{aligned}
\overline{m}_u(M_{Z'}) &= 0.00170 \text{ GeV}; & \overline{m}_c(M_{Z'}) &= 0.509 \text{ GeV}, \\
\overline{m}_t(M_{Z'}) &= 142.592 \text{ GeV}; & \overline{m}_d(M_{Z'}) &= 0.00342 \text{ GeV}; \\
\overline{m}_s(M_{Z'}) &= 0.0682 \text{ GeV}; & \overline{m}_b(M_{Z'}) &= 2.317 \text{ GeV}.
\end{aligned} \tag{20}$$

3.1 Z' decays in the extended model

To calculate the decay widths, we must include the additional exotic spectrum of the model from Sec. 2.2 in order to have a perturbative model at the required energy level. The partial decay widths of Z' into fermions $f\bar{f}$ at tree level are described by [17, 18]:

$$\Gamma_{Z' \rightarrow \bar{f}f}^0 = \frac{g_L^2 M_{Z'} N_c^f}{48\pi C_W^2} \sqrt{1 - \mu_f'^2} \left[\left(1 + \frac{\mu_f'^2}{2}\right) (\tilde{g}_v^f)^2 + (1 - \mu_f'^2) (\tilde{g}_a^f)^2 \right] R_{QED} R_{QCD}, \tag{21}$$

where $N_c^f = 1, 3$ for leptons and quarks, respectively, $R_{QED, QCD}$ are global final-state QED and QCD corrections, and $\mu_f'^2 = 4m_f^2/M_{Z'}^2$, takes into account kinematical corrections only important for the top quark. In order to calculate the corrections $R_{QED, QCD}$ defined in App. A, we use the running QED (α) and QCD (α_s) constants at the $M_{Z'}$ scale [15, 19]. We can also generate Z' decays into different flavors of quarks through the Lagrangian in Eq. 17, where at tree level

$$\Gamma_{Z' \rightarrow qq'}^0 = \frac{g_L^2 M_{Z'}}{16\pi C_W^2} \left[(\tilde{\mathfrak{g}}_v^{qq'})^2 + (\tilde{\mathfrak{g}}_a^{qq'})^2 \right] R_{QED} R_{QCD}. \tag{22}$$

The decays into heavy exotic particles $Z' \rightarrow K^+K^-, K^{++}K^{--}, \eta_3^+\eta_3^-, \rho_3^{++}\rho_3^{--}, J_j, E_j$ are suppressed because in this case we consider that only the effective THDM contributes, while the exotic particles are taken as heavy particles that are decoupled at energies below the scale μ_{331} . Decays into light bosons $Z' \rightarrow h^0h^0, Z_1\gamma, Z_1Z_1, Z_1h^0, W^+W^-$ which include the like-SM Higgs boson h^0 of the effective THDM are possible only through the small $Z - Z'$ mixing angle θ defined by Eq. 6, so that they are very suppressed, and do not contribute to the branching ratios in a significant amount [20]. Then, we do not take into account these decays in our analysis. On the other hand, since the oblique corrections are virtual processes sensitive to the heavy particles at any scale of energy, we must consider the one loop corrections to the Z' decay due to the exotic quarks J_j and leptons E_j at the scale $\mu_{331} \gtrsim M_{Z'}$. A detailed study of these corrections is performed in ref. [15] in the framework of models with $\beta = 1/\sqrt{3}$, where the Z' self-energy $\Sigma_{Z'Z'}$, the $Z' - Z$ vacuum polarization $\Pi_{Z'Z}$, and the Z' -photon vacuum polarization $\Pi_{Z'\gamma}$ (see the expressions in App. A) leads to the following decay width

$$\Gamma_{Z' \rightarrow \bar{f}f} = \Gamma_{Z' \rightarrow \bar{f}f}^0 (1 - \Delta'_f), \quad (23)$$

with

$$\Delta'_f \approx \frac{2(\tilde{g}_v^f \Delta \tilde{g}_v^f + \tilde{g}_a^f \Delta \tilde{g}_a^f)}{(\tilde{g}_v^f)^2 + (\tilde{g}_a^f)^2}, \quad (24)$$

that contains the oblique radiative corrections in $\Delta \tilde{g}_{v,a}^f$, which is defined as [15]

$$\begin{aligned} \Delta \tilde{g}_v^f &\approx 2S_W C_W Q_f \Pi_{Z'\gamma}(M_{Z'}^2) + g_v^f \Pi_{Z_2 Z_1}(M_{Z'}^2) \left(1 + \frac{M_Z^2}{M_{Z'}^2}\right) + \frac{1}{2} \tilde{g}_v^f \Sigma'_{Z'Z'}(M_{Z'}^2), \\ \Delta \tilde{g}_a^f &\approx g_a^f \Pi_{Z'Z}(M_{Z'}^2) \left(1 + \frac{M_Z^2}{M_{Z'}^2}\right) + \frac{1}{2} \tilde{g}_a^f \Sigma'_{Z'Z'}(M_{Z'}^2), \end{aligned} \quad (25)$$

where $\Sigma'_{Z'Z'} = d\Sigma_{Z'Z'}/dM_{Z'}^2$. The FCNC also exhibit corrections due to the Z' self-energy, where

$$\Gamma_{Z' \rightarrow qq'} = \Gamma_{Z' \rightarrow qq'}^0 (1 - \Delta'_{qq'}), \quad (26)$$

with

$$\Delta'_{qq'} \approx \frac{2(\tilde{g}_v^{qq'} \Delta \tilde{g}_v^{qq'} + \tilde{g}_a^{qq'} \Delta \tilde{g}_a^{qq'})}{(\tilde{g}_v^{qq'})^2 + (\tilde{g}_a^{qq'})^2}, \quad (27)$$

and

$$\Delta \tilde{g}_{v,a}^{qq'} \approx \frac{1}{2} \tilde{g}_{v,a}^{qq'} \Sigma'_{Z'Z'}(M_{Z'}^2). \quad (28)$$

With the above considerations, and taking into account the running coupling constants at the Z' resonance, we calculate the decay widths. Using the Eqs. 8 and 10 with the

	Γ_{ff} (GeV)			$Br(Z' \rightarrow ff) \times 10^{-2}$		
	A	B	C	A	B	C
$u\bar{u}$	73.862	73.862	119.967	13.622	13.635	25.891
$c\bar{c}$	73.862	119.967	73.862	13.622	22.146	15.940
$t\bar{t}$	119.962	73.325	73.325	22.124	13.536	15.825
$d\bar{d}$	34.211	34.211	81.097	6.309	6.315	17.502
$s\bar{s}$	34.211	81.097	34.211	6.309	14.971	7.383
$b\bar{b}$	81.097	34.211	34.211	14.956	6.315	7.383
$\ell^+\ell^-$	38.732			7.143	7.150	8.359
$\nu\bar{\nu}$	0.308			0.057	0.057	0.066

Table 6: *Partial widths and branching ratios of Z' into fermions at one loop level for each representation A, B, and C, in the framework of the EM. Leptons are universal of family.*

renormalization coefficients from Eq. 13 of the EM and the inputs from Eq. 12, we get at the $M_{Z'} \approx 4$ TeV scale that

$$\begin{aligned}
\alpha_Y^{-1}(M_{Z'}) &= 92.3468; & \alpha^{-1}(M_{Z'}) &= 118.305; \\
\alpha_2^{-1}(M_{Z'}) &= 25.9587; & \alpha_s^{-1}(M_{Z'}) &= 0.0779, \\
\overline{m}_t(M_{Z'}) &= 142.592; & S_W^2(M_{Z'}) &= 0.2194.
\end{aligned} \tag{29}$$

With the above values and considering $M_{J_j, E_j} = \mu_{331} \approx M_{Z'} = 4$ TeV, we obtain the widths shown in table 6 from Eq. 23, and in Tab. 7 for the FCNC contributions from Eq. 26. In the first case, values independent on the family representation (universal of family) are obtained for the leptonic sector in the two final rows in the table. In regard to the quark widths, we obtain the family dependent decays shown, so that we identify three bilepton models with the same particle content, but with observable differences. We also obtain the branching ratios of each decay, where we assume that only decays to SM particles are allowed, which is a reasonable approximation since other two body decays are very suppressed. In the FCNC contributions, we obtain very small values in the decay into the quarks uc and ut . However, we obtain that the flavor changing decay into the quarks ct and sb for the A and B models, are about the same order of magnitude as the diagonal components in Tab. 6, so that they contribute to the branching ratios. On the other hand, the model C suppresses most of the flavor changing effects of the neutral currents, which is also observed in models with $\beta = 1/\sqrt{3}$ [15] (Studies on the FCNC in 331 models are also carried out in refs. [20, 21, 22, 23, 24]).

3.2 Z' decays in the modified extended model

Now, we calculate the decay widths in the framework of the MEM from Sec. 2.3. However, we must take into account the new threshold defined by the exotic quarks J_j at 3 TeV, which modify the running QCD constant and the mass of the top quark at the Z' scale. Thus,

$\Gamma_{qq'}$ (GeV)	A-B	C
$Z' \rightarrow u\bar{c}$	5.00×10^{-4}	0
$Z' \rightarrow u\bar{t}$	5.00×10^{-4}	2.00×10^{-3}
$Z' \rightarrow c\bar{t}$	42.05	0
$Z' \rightarrow d\bar{s}$	1.91	7.65
$Z' \rightarrow d\bar{b}$	2.01	0
$Z' \rightarrow s\bar{b}$	40.02	0

Table 7: Partial width of Z' into quarks with FCNC for each representation A, B , and C , in the framework of the EM.

	Γ_{ff} (GeV)			$Br(Z' \rightarrow ff) \times 10^{-2}$		
	A	B	C	A	B	C
$u\bar{u}$	78.770	78.770	128.91	13.660	13.672	25.974
$c\bar{c}$	78.770	128.91	78.770	13.660	22.375	15.872
$t\bar{t}$	128.90	78.200	78.200	22.353	13.573	15.757
$d\bar{d}$	36.597	36.597	85.817	6.346	6.352	17.292
$s\bar{s}$	36.597	85.817	36.597	6.346	14.895	7.374
$b\bar{b}$	85.817	36.597	36.597	14.882	6.352	7.374
$\ell^+\ell^-$	41.733			7.237	7.243	8.409
$\nu\bar{\nu}$	0.310			0.054	0.054	0.062

Table 8: Partial widths and branching ratios of Z' into fermions at one loop level for each representation A, B , and C , in the framework of the MEM. Leptons are universal of family.

with the inputs from Eq. 16, we obtain at $M_{Z'} \approx 4$ TeV

$$\begin{aligned}
\alpha_Y^{-1}(M_{Z'}) &= 67.229; & \alpha^{-1}(M_{Z'}) &= 101.377; \\
\alpha_2^{-1}(M_{Z'}) &= 22.5224; & \alpha_s(M_{Z'}) &= 0.0791, \\
\overline{m}_t(M_{Z'}) &= 142.579; & S_W^2(M_{Z'}) &= 0.2222
\end{aligned} \tag{30}$$

Comparing with Eq. 29, we note the strong dependence of the running constants with the particle content. The running masses of the other quarks do not present an appreciable change respect the values given by Eq. 20. Taking into account the one loop corrections with $M_{J_j, E_j} = 3$ TeV, we obtain the widths from Eq. 23 and the branching ratios shown in Tab. 8. Although the decays $Z_2 \rightarrow K^+K^-, K^{++}K^{--}, \eta_3^+\eta_3^-, \rho_3^{++}\rho_3^{--}, J_j, E_j$ are not forbidden if we download all the exotic spectrum at the TeV scales, they are very suppressed by kinematical factors [20]. Table 9 show the FCNC widths for this case.

3.3 Discussion

The results of the decay widths and branching ratios show observable differences between the representation A, B and C , thus each case from Table 2 define three models that leads to

$\Gamma_{qq'}$ (GeV)	A-B	C
$Z' \rightarrow u\bar{c}$	5.20×10^{-4}	0
$Z' \rightarrow u\bar{t}$	5.20×10^{-4}	2.53×10^{-3}
$Z' \rightarrow c\bar{t}$	43.63	0
$Z' \rightarrow d\bar{s}$	1.98	9.36
$Z' \rightarrow d\bar{b}$	2.08	0
$Z' \rightarrow s\bar{b}$	41.51	0

Table 9: *Partial width of Z' into quarks with FCNC for each representation A,B, and C for the MEM*

different predictions of the extra neutral boson Z' . Then, the assignation of the phenomenological quarks into the 331 representations define 3 different bilepton models with the same particle content.

Comparing the above results with other estimations performed in the framework of models with $\beta = 1/\sqrt{3}$ [15] and bilepton models [20], we get partial widths about one order of magnitude bigger for the quark sector and the charged lepton sector, while the neutrinos results one order of magnitude smaller. These differences in the partial widths may be used in order to distinguish which 331 model could describe in a better way the physics at the TeV energy scale in the future experiments. The branching ratios are in the range $10^{-2} \leq Br(Z_2 \rightarrow qq) \leq 10^{-1}$ for quarks, $Br(Z_2 \rightarrow \ell^+\ell^-) \approx 10^{-2}$ for the charged leptons, and $Br(Z_2 \rightarrow \nu\nu) \approx 10^{-4}$ for neutrinos. Comparing with the model $\beta = 1/\sqrt{3}$ [15] or the bilepton model from ref. [20], we get branching ratios between one and two order of magnitude smaller.

On the other hand, by comparing Tables 6 and 8, we get that the modified extended particle content predict widths about 6 % bigger that extended bilepton model. In general, we see that each decay width increase when exotic particles, in particular when the exotic quarks of the minimal bilepton model are downloaded below the Z' resonance. The branching ratios present very similar values between both particle contents, so that the additional effects of the new threshold an the presence of additional exotic particles are canceled in the calculations of the ratios. Just as the top quark contribute to the one loop Z decay, the above decay widths were calculated at one loop level throught the heavy particles J_j and E_j , where we take into account the running coupling constant at the $M_{Z'}$ energy level.

The branching ratios receive important contributios to the flavor changing decays $Z' \rightarrow ct, sb$ in the A and B models. The other flavor changing effects are very small, in particular, the FCNC phenomenology is practically absent for C models, as can be seen in Tabs. 7 and 9.

4 Conclusions

In this work we studied the main contributions of the Z' decay in the framework of the 331 bilepton model with extra particles that pull the Landau pole beyond the TeV scale energies in order to get a perturbative model at the Z' peak. These calculations were performed for two different particle contents, first in the model proposed in ref. [12] where three lepton triplets with null hypercharge, one scalar triplet with null hypercharge and two scalar doublets with $Y^2 = 9$ remains as new degrees of freedom at energies below $M_{Z'}$, and later in a modified extended model (MEM) where the full 331 spectrum from tables 1 and 3 is taken into account with a degenerated exotic spectrum at 3 TeV in agreement with some phenomenological studies [13]. In particular, the presence of the exotic quarks J_j as an active degree of freedom below the Z' scale, define a new threshold that change the evolution of the running parameters. In general, we obtained predictions for 6 different perturbative models with two particle contents. As seen in tables 6-9, each case A , B and C from Tab. 2 lead to different predictions of the Z' decays, thus they represent three different bilepton model. The width decays obtained are of the order of 10^2 GeV for quarks and charged leptons which are one order of magnitude bigger than the predicted by the models with $\beta = 1/\sqrt{3}$, while the decays into neutrinos are of the order 10^{-1} , one order of magnitude smaller than in models $\beta = 1/\sqrt{3}$. We also obtained the branching ratios, where decays into exotic particles are not taken into account by kinematical reasons and decays into light bosons are suppressed by the small $Z - Z'$ mixing angle. However, FCNC effects through the ansatz of Matsuda on the texture of the quark mass matrices leads to important contribution in the decays $Z' \rightarrow ct, sb$, which are of the order of 10^2 GeV and should be taken into account in the total decay width.

We acknowledge financial support from Colciencias. We also thanks to HELEN (High Energy Physics LatinAmerican - European Network) Program

Appendix

A Radiative Corrections

The Z' decay in Eq. (21) contains global QED and QCD corrections through the definition of $R_{QED} = 1 + \delta_{QED}^f$ and $R_{QCD} = 1 + (1/2)(N_c^f - 1)\delta_{QCD}^f$, where [17, 18]

$$\begin{aligned}\delta_{QED}^f &= \frac{3\alpha Q_f^2}{4\pi}; \\ \delta_{QCD}^f &= \frac{\alpha_s}{\pi} + 1.405 \left(\frac{\alpha_s}{\pi}\right)^2 - 12.8 \left(\frac{\alpha_s}{\pi}\right)^3 - \frac{\alpha\alpha_s Q_f^2}{4\pi^2}\end{aligned}\quad (31)$$

with α and α_s the electromagnetic and QCD constants, respectively. The values α and α_s are calculated at the $M_{Z'}$ scale as shown in Eqs. 29 and 30 in agreement with each particle content and quark thresholds [19].

The correction due to the Z' self-energy leads to the wavefunction renormalization

$$Z' \rightarrow Z'_R \approx \left(1 - \frac{1}{2} \Sigma_{Z'Z'}^{(fin)'}(q^2)\right) Z', \quad (32)$$

which is sensitive to the heavy fermions $f_j = J_j, E_j$, where

$$\begin{aligned} \Sigma_{Z'Z'}^{(fin)'}(q^2) &= \frac{d\Sigma_{Z'Z'}^{(fin)}}{dq^2} = \frac{1}{12\pi^2} \left(\frac{g_L}{2C_W}\right)^2 \sum_{f_j} \left\{ (\tilde{g}_v^{f_j})^2 \left(\frac{2}{3} - \ln \frac{m_{f_j}^2}{q^2}\right) \right. \\ &\quad \left. + (\tilde{g}_a^{f_j})^2 \left(\frac{2}{3} - \ln \frac{m_{f_j}^2}{q^2} - \frac{6m_{f_j}^2}{q^2}\right) \right\}. \end{aligned} \quad (33)$$

The $Z' - Z$ self-energy leads to the following vacuum polarization

$$\begin{aligned} \Pi_{Z'Z}^{(fin)}(q^2) &\approx \frac{1}{12\pi^2} \left(\frac{g_L}{2C_W}\right)^2 \sum_{f_j} \left\{ \tilde{g}_v^{f_j} g_v^{f_j} \left[-\ln \frac{m_{f_j}^2}{q^2} - \frac{1}{3}\right] \right. \\ &\quad \left. + \tilde{g}_a^{f_j} g_a^{f_j} \left[\left(\frac{6m_{f_j}^2}{q^2} - 1\right) \ln \frac{m_{f_j}^2}{q^2} - \frac{1}{3}\right] \right\}, \end{aligned} \quad (34)$$

and the Z' -photon vacuum polarization is given by

$$\Pi_{Z'\gamma}^{(fin)}(q^2) \approx \frac{1}{12\pi^2} \frac{g_L^2 S_W}{2C_W} \sum_{f_j} \left\{ Q_{f_j} \tilde{g}_v^{f_j} \left[-\ln \frac{m_{f_j}^2}{q^2} - \frac{1}{3}\right] \right\}, \quad (35)$$

with Q_{f_j} the electric charge of the virtual f_j fermions given in table 1.

References

- [1] J.S. Bell, R. Jackiw, *Nuovo Cim.* **A60** 47 (1969); S.L. Adler, *Phys. Rev.* **177**, 2426 (1969); D.J. Gross, R. Jackiw, *Phys.Rev.* **D6** 477 (1972). H. Georgi and S. L. Glashow, *Phys. Rev.* **D6** 429, (1972); S. Okubo, *Phys. Rev.* **D16**, 3528 (1977); J. Banks and H. Georgi, *Phys. Rev.* **14** 1159 (1976).
- [2] S. Godfrey in *Proc. of the APS/DPF/DPB Summer Study on the Future of Particle Physics (Snowmass 2001)*, ed. N. Graf, arXiv: hep-ph/0201093 and hep-ph/0201092; Marcela Carena, Alejandro Daleo, Bogdan A. Dobrescu, Tim M.P. Tait, *Phys. Rev.* **D70**, 093009 (2004); G. Weiglein et. al. LHC/LC Study Group, arXiv: hep-ph/0410364
- [3] P.H. Frampton, P.Q. Hung and M. Sher, arXiv: hep-ph/9903387 v2.
- [4] C.A.deS. Pires and O.P. Ravinez, *Phys. Rev.* **D58**, 35008 (1998); C.A.deS. Pires, *Phys. Rev.* **D60**, 075013 (1999).

- [5] L.A. Sánchez, W.A. Ponce, and R. Martínez, Phys. Rev. **D64**, 075013 (2001).
- [6] R. Foot, H.N. Long and T.A. Tran, Phys. Rev. **D50**, R34 (1994); H.N. Long, Phys. Rev. **D53**, 437 (1996); *ibid*, **D54**, 4691 (1996); H.N. Long, Mod. Phys. Lett. **A13**, 1865 (1998).
- [7] F. Pisano and V. Pleitez, Phys. Rev. **D46**, 410 (1992); P.H. Frampton, Phys. Rev. Lett. **69**, 2889 (1992); P.H. Frampton, P. Krastev and J.T. Liu, Mod. Phys. Lett. **9A**, 761 (1994); P.H. Frampton et. al. Mod. Phys. Lett. **9A**, 1975 (1994); Nguyen Tuan Anh, Nguyen Anh Ky, Hoang Ngoc Long, Int. J. Mod. Phys. **A16**, 541 (2001).
- [8] Rodolfo A. Diaz, R. Martinez, F. Ochoa, Phys. Rev. **D69**, 095009 (2004).
- [9] Rodolfo A. Diaz, R. Martinez, F. Ochoa, Phys. Rev. **D72**, 035018 (2005).
- [10] Fredy Ochoa and R. Martinez, Phys. Rev. **D72**, 035010 (2005).
- [11] A.G. Dias, R. Martínez and V. Pleitez, Eur. Phys. J. **C39**, 101-107 (2005).
- [12] A.G. Dias, Phys. Rev. **D71**, 015009 (2005).
- [13] G.A. González-Sprinberg, R. Martínez and O. Sampayo, Phys. Rev. **D71**, 115003 (2005).
- [14] In this connection see K.T. Mahanthappa and P.K. Mohapatra, Phys. Rev. **D42**, 1732-2400 (1990); Phys. Rev. **D43**, 3093 (1991).
- [15] A. Carcamo, R. Martinez and F. Ochoa, Phys. Rev. **D73**, 035007 (2006).
- [16] K. Matsuda, H. Nishiura, Phys. Rev. **D69**, 053005 (2004)
- [17] S. Eidelman et. al. Particle Data Group, Phys. Lett. **B592**, (2004), pp. 120-121.
- [18] J. Bernabeu, A. Pich and A. Santamaria, Nucl. Phys. **B363** (1991) 326; D. Bardin et.al. Electroweak Working Group Report, arXiv: hep-ph/9709229 (1997) 28-32.
- [19] H. Fusaoka and Y. Koide, Phys. Rev. **D57**, 3986 (1998).
- [20] M.A. Perez, G. Tavares-Velasco and J.J. Toscano, Phys. Rev. **D69**, 115004 (2004)
- [21] M.A. Perez, M.A. Soriano, Phys. Rev. **D46**, 125 (1992).
- [22] Ambar Ghosal, Y. Koide, H. Fusaoka, Phys. Rev. **D64**, 053012 (2001); J.I. Illana, T. Riemann, Phys. Rev **D63**, 053004 (2001); D. Delepine, F. Vissani, Phys. Lett. **B522**, 95-101 (2001); T. Rador, Phys. Rev. **D59**, 095012 (1999).
- [23] Paul Langacker, M. Plumacher, Phys. Rev. **D62**, 013006 (2000); V. Barger, Cheng-Wei Chiang, P. Langacker, Hye-Sung Lee, Phys. Lett. **B580**, 186-196 (2004); S. Fajfer, P. Singer, Phys. Rev. **D65**, 017301 (2002).

- [24] D.L. Anderson and M. Sher, Phys. Rev. **D72**, 095014 (2005); J. A. Rodriguez and M. Sher, Phys. Rev. **D70** 117702 (2004).
- [25] W. Bernreuther and W. Wetzel, Nucl. Phys. **B197**, 228 (1982); W. Bernreuther, Ann. Phys.**151**, 127 (1983); K.G. Chetyrkin, B.A. Kniehl and M. Steinhauser, Phys. Rev. Lett. **79**, 2184 (1997).

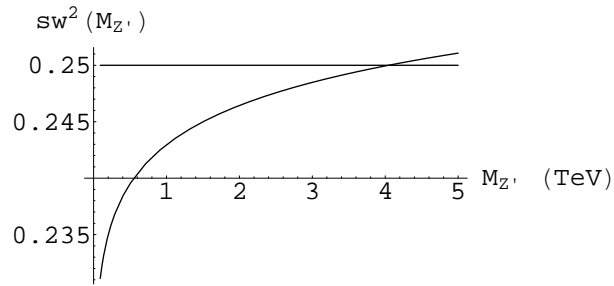


Figure 1: Running Weinberg angle for the minimal 331 bilepton model (MM) in the framework of the effective THDM (without exotic particles). A Landau-like pole is found at the $M_{Z'} \approx 4$ TeV energy scale

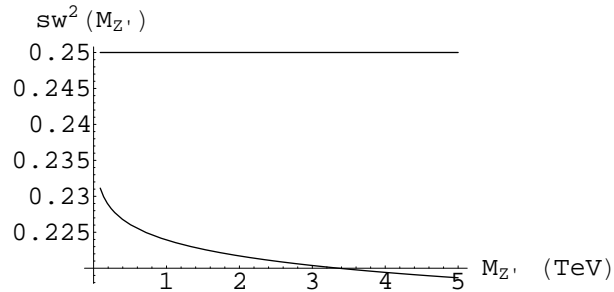


Figure 2: Running Weinberg angle for the extended 331 bilepton model (EM) with a new set of leptonic particles. The angle show decreasing behavior, from where the Landau pole is avoid

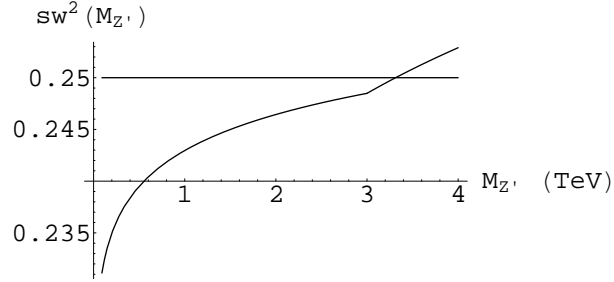


Figure 3: Running Weinberg angle for the MM with exotic particles at the 3 TeV threshold below $M_{Z'}$. A Landau-like pole is found at 3.5 TeV energy scale

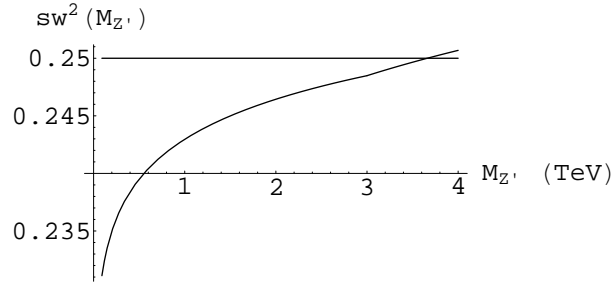


Figure 4: Running Weinberg angle for the modified extended model (MEM) with the full exotic spectrum of the MM and EM at the 3 TeV threshold. A Landau-like pole is found at the $M_{Z'} \approx 3.7$ TeV energy scale

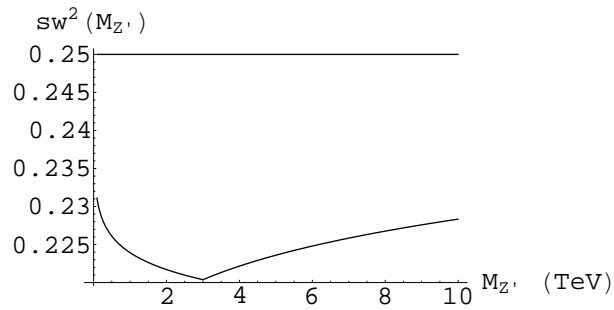


Figure 5: Running Weinberg angle for the MEM with the new leptonic particles running below the 3 TeV threshold defined by the minimal exotic spectrum. A Landau-like pole is pulled far away from the TeV energy scales.